Journal of Engineering and Applied Sciences 12 (20): 5286-5293, 2017
ISSN: 1816-949X

Meshless Point Interpolation Formulation of Kinematic Wave Equation for Flood Routing

[1]H. Hirol, [1]M.A. Mohd Noor, [1]E.H. Kasiman, [1]A.K.B. Hong,
[1]Z. Yusop and [2]A.Y. Mohd Yassin
[1]Faculty of Civil Engineering, University Teknologi Malaysia,
81310 Johor Bahru, Johor, Malaysia
[2]Department of Civil and Environmental Engineering, University Teknologi Petronas,
32610 Bandar Seri Iskandar, Perak, Malaysia

Abstract: This study presents the meshless Point Interpolation Method (PIM) formulation to solve kinematic wave equation for flood routing. It details on Galerkin residual method employing PIM shape functions in discretizing the unsteady partial differential equation. Two nonlinear solvers are considered; Picard and Newton-Raphson. The formulation are verified against both hypothetical data obtained from conventional numerical methods (finite difference and finite element method) and gauged data obtained from an actual river. Close agreements are obtained between the proposed PIM formulation and the conventional methods thus highlight the potential of PIM as an alternative numerical method in the field of hydrologic modelling.

Key words: Meshless method, point interpolation method, finite difference method, finite element method, Saint Venant kinematic wave equation, hydrologic modelling

INTRODUCTION

The hydrologic phenomenon of surface runoff and channel flow can be approximately predicted by solving a set of one-dimensional nonlinear unsteady partial differential equations known as St. Venant equations. The equations consist of continuity and momentum equations which can be further classified into full dynamics, diffusive and kinematic wave equations. Full dynamics equations allow for complete description of the flow, whilst diffusive equations able to capture backwater effect. If the slope of the plane is assumed to be equal to the frictional slope, the continuity equation and the momentum equation can be uncoupled and hence the prevalence of the kinematic wave equation.

Due to its simplicity, kinematic wave has been conveniently applied in various hydrologic modelling such as watershed runoff, flood routing in rivers, channel flows, erosion and sediment transports (Singh, 2003). However, despite being the simplest case of St. Venant equations there is no closed form solution available for the kinematic wave except for the very simplified cases as worked by Hjelmfelt (1981), Parlange *et al.* (1981) and Govindaraju *et al.* (1988, 1990). The difficulty is due to the nonlinearity as well as the unsteady nature of the equation. Therefore, at present in obtaining the solution for the more general cases, kinematic wave equation is commonly solved numerically using Finite Difference Method (FDM) (Chow *et al.*, 1988) or finite element method as by Vieux *et al.* (1990) and Litrico *et al.* (2010).

MATERIALS AND METHODS

Point Interpolation Method (PIM): A meshless method: Meshless methods can be considered as the latest output in the research and development of numerical techniques. The discoveries were motivated by the attempt to remove the need for predefined meshes of FEM. It is argued that with the removal of the mesh, computer cost in the Mesh development as well as in mesh refinement can be reduced. Since, there could be various ways in doing this, meshless methods do not refer to a specific method but to a family of methods. Point Interpolation Method (PIM) is one that falls under this family.

PIM uses polynomial functions as the basis for the derivation of the shape functions. This differs from other Meshless methods such as Radial Point Interpolation Method (RPIM) that uses radial basis functions and Element Free Galerkin (EFG) that uses moving least square functions, just to name a few. The method was first proposed by Liu and Gu (1999) before enhanced by Liu and Gu (2003, 2004) and Liu *et al.* (2004).

Despite the various works and formulations of FDM and FEM on kinematic wave equation there is yet a PIM

Corresponding Author: H. Hirol, Faculty of Civil Engineering, Universiti Teknologi Malaysia, 81310 Johor Bahru, Johor, Malaysia

formulation for the problem. Such an undertake is thus, important as, not only it can provide alternative numerical method in the field of flood routing but also assist in the establishment of Meshless methods within the field of civil engineering by widening the application of the methods into hydrology and river engineering. It is therefore the main interest of this study to present the formulation of PIM meshless method and its verification to flood routing problems based on kinematic wave assumption.

Governing equations: Saint Venant equations are time dependent partial differential equations which describe the distribution of flow rate, Q and flow cross-sectional area, A as functions of distance, x along the channel and time t. The equations were first derived by Barre de Saint-Venant in 1871 (Vieux *et al*., 1990). The equations were derived by considering the two conservation laws which are the conservation of mass and the conservation of momentum. The final forms of the partial differential equations are given as follows.

Equation of mass:

$$\frac{\partial A}{dt}+\frac{\partial Q}{\partial x}=q(x) \tag{1}$$

Where:

A = The cross-sectional area of the flow
Q = The flow rate
q (x) = The forcing term (i.e., precipitation, lateral flow)

Equation of momentum:

$$\frac{1}{A}\frac{\partial Q}{\partial t}+\frac{1}{A}\frac{\partial}{\partial x}\left(\frac{Q^2}{A}\right)+g\frac{\partial y}{\partial x}-g(S_o-S_f)=0 \tag{2}$$

Where:

S_0 = The bed slope
S_f = The frictional slope
y and g = The depth of water and gravitational pull, respectively

The complete form of Eq. 2 is termed as full dynamics equation. If the first two terms on the left hand side of the equation are omitted, we then obtain diffusive equation.

However, Eq. 2 can be further simplified if it is assumed that $S_o = S_F$. This is known as the kinematics wave assumption. This condition can be equivalently treated in Manning form as:

$$A=\alpha Q^{\beta} \tag{3}$$

Equation 1 and 3 are the Saint Venant kinematic wave equations. By combining Eq. 1 and 3, the following equation can be obtained:

$$\frac{\partial Q}{\partial t}+\frac{1}{\alpha\beta}Q^{(1-\beta)}\frac{\partial Q}{\partial x}=q \tag{4}$$

Weak form of kinematic wave: The kinematic wave equation given as Eq. 4 can be solved numerically by converting the equation into weak form. This can be done by employing Galerkin weighted residual method. We first discretize Eq. 4 in time by forward-difference to obtain:

$$\frac{Q^{t+1}-Q^{t}}{\Delta t}+\frac{1}{\alpha\beta}Q^{(1-\beta),t+1}\frac{\partial Q^{t+1}}{\partial x}=q^{t+1} \tag{5}$$

where, t+1 and t refers to present and previous time-step, respectively. Rearranging gives:

$$Q^{t+1}+\frac{\Delta t}{\alpha\beta}Q^{(1-\beta),t+1}\frac{\partial Q^{t+1}}{\partial x}-Qt=q^{t+1} \tag{6}$$

By weighting Eq. 6 by shape functions, and expressing the flow rate as where are the degree of freedoms or the nodal values of the following is obtained:

$$\int_L N_i\left(N_jQ_j+\frac{\Delta t}{\alpha\beta}N_kQ_k^{(1-\beta)}\frac{\partial N_jQ_j}{\partial x}-N_jQ_j^{t}\right)dx=\int_L N_iqdx \tag{7}$$

To note, in Eq. 7, superscript t+1 is omitted for ease of notation. By collecting the degree of freedoms, Q_j and shifting known terms to the right hand side of Eq. 7 can now be given as:

$$\left(\int_L N_iN_jdx+\int_L\frac{\Delta t}{\alpha\beta}N_i\left(N_kQ_k\right)^{(1-\beta)}\frac{\partial N_j}{\partial x}dx\right)$$
$$Q_j=\int_L N_iN_jQ_j^{t}dx+\int_L N_iqdx \tag{8}$$

In indicial notation, Eq. 8 can be represented as:

$$\left(M_{ij}+K_{ij}\right)Q_j=-F_i \tag{9}$$

or in matrix form as:

$$\left[M+K(Q)\right]\{Q\}=-\{F\} \tag{10}$$

Where:

K_{ij} or [K] = The stiffness matrix
M_{ij} or [M] = The mass matrix whilst Q_j or {Q}
F_i or {F} = The vector of degree of freedom and load, respectively

Each can be given as:

$$[M] = M_{ij} = \int_L N_i N_j \, dx \quad (11)$$

$$[K(Q)] = K_{ij} = \int_L \frac{\Delta t}{\alpha\beta} N_i (N_k Q_k)(1-\beta)\frac{\partial N_j}{\partial x} dx \quad (12)$$

$$\{F\} = F_i = \int_L N_i N_j Q_j^t \, dx + \int_L N_i \, q dx \quad (13)$$

Nonlinear solvers: Equation 9 and 10 is nonlinear thus requires nonlinear solvers. In this research, two nonlinear solvers have been employed then verified; Picard's and Newton-Raphson scheme. Each of the scheme is detailed next.

Picard's scheme: Picard scheme is also known as the direct substitution iteration method. It is called direct because the scheme involves direct substitution of initial (or previous) solved degree of freedoms into the stiffness matrix in solving the current ones and this process is iterated until the solution is converged. But such simplicity usually works only for mild nonlinear problems but diverges for severe nonlinearity.

Newton-Raphson's scheme: An alternative iterative scheme which performs better when the nonlinearity is more severe is the Newton-Raphson scheme. The basic concept of the scheme is based on the Taylor series expansion. The residual of the equilibrium equations can be given as:

$$\{R(Q)\} \equiv [M+K(Q)]\{Q\} - \{F\} \quad (14)$$

Expanding Eq. 14 by Taylor series about the known $(r-1)^{th}$ solution gives:

$$\{R(Q)^{r-1}\} + \frac{\partial\{R(Q)^{r-1}\}}{\partial\{Q\}^{r-1}}\{\Delta Q\} = 0 \quad (15)$$

where, the series has been truncated up to linear terms only. Rearranging gives:

$$\frac{\partial\{R(Q)^{r-1}\}}{\partial\{Q\}^{r-1}}\{\Delta Q\} = -\{R(Q)^{r-1}\} \quad (16)$$

By defining a new matrix, termed as tangent stiffness matrix, $[T(Q)^{r-1}]$:

$$[T(Q)^{r-1}] = \frac{\partial\{R(Q)^{r-1}\}}{\partial\{Q\}^{r-1}} \quad (17)$$

Equation 17 can be compactly given as:

$$[T(Q)^{r-1}]\{\Delta Q\} = -\{R(Q)^{r-1}\} \quad (18)$$

Examining Eq. 18, one can observe that $\{\Delta Q\}$ is now solvable since the other terms, i.e. $[T(Q)^{r-1}]$ and $[T(Q)^{r-1}]$ are now known from the previous iteration, i.e. $(R-1)^{th}$. By inversing $[T(Q)^{r-1}]$, $\{\Delta Q\}$ is thus obtained as:

$$\{\Delta Q\} = [T(Q)^{r-1}]^{-1}\left(-\{R(Q)^{r-1}\}\right) \quad (19)$$

Once $\{\Delta Q\}$ is solved, the solution at the rth iteration is updated thus:

$$\{Q\}^r = \{Q\}^{r-1} + \{\Delta Q\} \quad (20)$$

In the next iteration, $\{Q\}^r$ of Eq. 20 is inserted back into Eq. 19 and take the role of $\{Q\}^{r-1}$ in the determination of $[T(Q)^{r-1}]$ and $\{R(Q)^{r-1}\}$. This process is repeated until the solution converges.

Point Interpolation Method (PIM): The main difference between FEM and Meshfree formulation is in the derivation of the shape function. To the knowledge of this study, no work on Meshfree formulation employing PIM shape functions in solving kinematic wave has ever been reported.

Point Interpolation Method (PIM) shape functions: PIM shape functions use polynomial as the interpolation functions. Consider a distribution of flow arte Q(x) in a one dimensional flow region discretized by a set field nodes. Interpolation of Q(x) by polynomial can be represented as:

$$Q = \{P\}\{a\}^T = P_m a_m \quad (21)$$

Where:

{P} = The monomials built from Pascal triangle
m = The number of the polynomial terms
{a} = The vector of coefficient which both having the size of 1×m

{P} and {a} are given as:

$$\{P\} = P_m = \{1, x, x^2, ..., x^{m-1}\} \quad (22)$$

$$\{a\} = a_m = \{a_1, a_2, a_3, ..., a_m\} \quad (23)$$

The coefficient a_m in Eq. 23 can be determined by enforcing the functions to go precisely through the nodal values of the n nodes. In matrix forms this equation can be written as:

$$\{Q\}^T = [P|_n]\{a\}^T \quad (24)$$

Where:

{Q} = The vector of the nodal values of the flow rate (or also known as the vector of degree of freedom)

$[P|_n]$ = Contains the evaluated values of the monomials when evaluated at the location of the nodes (i.e., x_n) which can be given as:

$$[P|_n] = \begin{bmatrix} 1 & x_1 & x_1^2 \ldots & x_1^{m-1} \\ 1 & x_2 & x_2^2 \ldots & x_2^{m-1} \\ 1 & x_3 & x_3^2 \ldots & x_3^{m-1} \\ . & . & . & . \\ . & . & . & . \\ 1 & x_n & x_n^2 \ldots & x_n^{m-1} \end{bmatrix} \quad (25)$$

$[P|_n]$ is called the moment matrix. As can be noticed in Eq. 24 is a constant matrix. From Eq. 24 by inversing the moment matrix $[P|_n]$, we can solve for {a}. This is given as:

$$\{a\}^T = [P|_n]^{-1}\{Q\}^T \quad (26)$$

By inserting Eq. 26 back into Eq. 24 we obtain:

$$Q = \{P\}[P|_n]^{-1}\{Q\}^T \quad (27)$$

Equation 27 can then be expressed as:

$$Q = \{N\}\{Q\}^T = N_m Q_m \quad (28)$$

where, {N} or N_m are the PIM shape functions hence, its derivation. The shape functions can be shown to have the Kronecker delta property as follows:

$$N_j(x = x_m) = 1 \quad j = m \quad (29)$$

$$N_j(x = x_m) = 1 \quad j = m \quad (30)$$

Due to this property, the essential boundary conditions can be easily imposed in PIM.

Evaluated values of PIM shape functions: Derivation of PIM shape functions given above is based on the direct inversion of the moment matrix $[P|_n]$ (i.e. $[P|_n]^{-1}$). However, this is not the practice of many Meshfree formulations. Instead, the coefficients {a} are solved by Gauss elimination which is made possible by evaluating both the polynomial interpolation (i.e., Eq. 21) and the shape function interpolation (i.e., Eq. 28) at a point of interest (i.e., Gauss points) and then equating them. This is detailed as follows.

Since Eq. 21 and 27 represent the same distribution of the flow rate, the equations should give the same value when evaluated at the same location (i.e., point of interest). This gives:

$$\{N|_{pi}\}\{Q\}^T = \{P|_{pi}\}\{a\}^T \quad (31)$$

where, subscript p_i means point of interest. Inserting Eq. 24 gives:

$$\{N|_{pi}\}[P|_n]\{a\}^T = \{P|_{pi}\}\{a\}^T \quad (32)$$

After cancellation of $\{a\}^T$ and some rearrangement, Eq. 32 can be given as:

$$[P|_n]^T\{N|_{pi}\}^T = \{P|_{pi}\}^T \quad (33)$$

By solving in Eq. 33, the shape functions at a point of interest can be obtained by employing simultaneous equation solver such as Gauss elimination thus avoid the need for direct inversion.

First derivative of PIM shape functions: As can be seen in Eq. 4, the kinematic wave equation has first derivative term. Derivative of the PIM shape functions is determined as follows.

Differentiating Eq. 28 and 21 and evaluating at a point of interest, we obtain:

$$\left\{\left.\frac{\partial N_1}{\partial x}\right|_{pi} \left.\frac{\partial N_2}{\partial x}\right|_{pi}, \ldots, \left.\frac{\partial N_n}{\partial x}\right|_{pi}\right\}\begin{Bmatrix} Q_1 \\ Q_2 \\ \vdots \\ Q_n \end{Bmatrix} = \{0\ 1, \ldots, (n-1)x^{n-2}\}\begin{Bmatrix} a_1 \\ a_2 \\ \vdots \\ a_n \end{Bmatrix} \quad (34)$$

which can be compactly given as:

$$\{\partial N|_{pi}\}\{Q\}^T\{\partial P|_{pi}\}\{a\}^T \quad (35)$$

Where:

$$\{\partial N|_{pi}\} = \left\{\left.\frac{\partial N_1}{\partial x}\right|_{pi} \left.\frac{\partial N_2}{\partial x}\right|_{pi}, \ldots, \left.\frac{\partial N_n}{\partial x}\right|_{pi}\right\} \quad (36)$$

$$\{\partial P|_{pi}\} = \{0\ 1, ..., (n-1)x^{n-2}\} \quad (37)$$

Inserting Eq. 24 into Eq. 35 gives:

$$\{\partial N|_{pi}\}[P|_n]\{a\}^T = \{\partial P|_{pi}\}\{a\}^T \quad (38)$$

Cancelling $\{a\}^T$ and some rearranging, we obtain:

$$[P|_n]^T \{\partial N|_{pi}\}^T = \{\partial P|_{pi}\} \quad (39)$$

Solving for $\{\partial N|_{pi}\}$, we obtain the evaluated values of the derivative of the PIM shape functions at the location of the point of interest.

Final form of kinematic wave PIM formulation: Inserting $\{N|_{pi}\}$ of Eq. 33 and $\{\partial N|_{pi}\}$ of Eq. 39 into the descritized weak formulation of Eq. 11-13, the final form of PIM formulation of the kinematic wave can be given as (in numerical integration forms):

$$[M] = M_{ij} \sum_{f=1}^{BC}\sum_{g=1}^{GP} \widehat{W}_g N_i|_g\, N_j|_g |J_f| \quad (40)$$

$$[K] = K_{ij} = \sum_{f=1}^{BC}\sum_{g=1}^{GP} \widehat{W}_g \frac{\Delta t}{\alpha\beta} N_i|_g \left(N_k|_g\, Q_k|_g\right)^{(1-\beta)} \frac{\partial N_j|_g}{\partial x} |J_f| \quad (41)$$

$$\{F\} = F_i = \sum_{f=1}^{BC}\sum_{g=1}^{GP} \widehat{W}_g \left[N_i|_g\, N_j|_g\, Q_j + N_i|_g\, q\right] |J_f| \quad (42)$$

$$[T] = T_{ij} = \sum_{f=1}^{BC}\sum_{g=1}^{GP} \widehat{W}_g \left[\begin{array}{l} N_i|_g\, N_j|_g + (2-\beta)\dfrac{\Delta t}{\alpha\beta} N_i|_g \\ \left(N_k|_g\, Q_k|_g\right)^{(1-\beta),r-1} \dfrac{\partial N_j|_g}{\partial x} \end{array}\right] |J_f| \quad (43)$$

Where:

$|J_f|$ = The Jacobian for fth background cell
$\widehat{w}_g$ = The Gauss weighting factor for the gth Gauss point
GP = The total number of gauss points
BC = The background cell of the gauss quadrature

RESULTS AND DISCUSSION

Verifications of formulation

Case 1: Verification against Chow *et al.* (1988): The first verification is made against the numerical solution obtained from FDM of Chow *et al.* (1988). The flow is driven by a time-varying inflow as given in Table 1. The hypothetical channel discretized into a finite grid system is shown in Fig. 1. The channel has a bed slope of one percent and a Manning's roughness factor of 0.035. There is no lateral inflow (precipitation). The initial condition is a uniform flow of 2000 cfs along the channel.

Table 1: Chow *et al.* (1988) input data

Inflow time (min) (1)	Inflow rate (cfs) (2)
0	2000
12	2000
24	3000
36	4000
48	5000
60	6000
72	5000
84	4000
96	3000
108	2000
120	2000

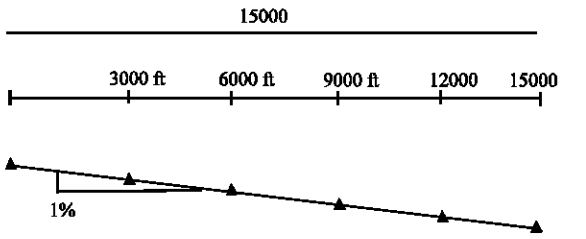

Fig. 1: Uniformly distributed discretization points along the channel (Chow *et al.*, 1988)

Two spatial points have been chosen for comparison purposes; 6000 and 12000 ft measured from upstream. The plots of flow rate, Q versus time, t are shown in Fig. 2-5 for various node refinement and for the two nonlinear schemes. The close agreement between the results verifies the PIM formulations.

Case 2: Verification against Vieux *et al.* (1990): In Case 1, precipitation or rainfall is not considered. To allow for such a forcing term, verification is made against results detailed by Vieux *et al.* (1990). Also, whilst Chow *et al.* (1988) employed FDM, Vieux *et al.* (1990). Employed FEM as the numerical method. Figure 6 shows the hypothetical watershed considered by Vieux *et al.* (1990). In contrast to Case 1 and as can be seen in Fig. 6, varying slope is allowed where the upper plane has a slope of 6% whilst the lower plane has a slope of 3%. At midpoint point where planes with different slope intersected, averaged value of the slopes, i.e., 4.5%. The length of the plane is 200 ft. The flow is subjected to a constant intensity precipitation (rainfall) with an intensity of 1.097 cm/h (0.00001 ft/sec). The Manning roughness coefficient is taken as 0.035 at each node. Various numbers of elements was considered for convergence study purposes (i.e., 2, 20 and 50 elements).

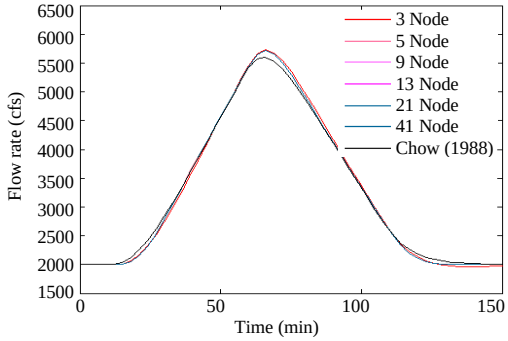

Fig. 2: Flow rate at point 6000 ft obtained by Newton-Raphson PIM; Newton PIM at node 6000 ft

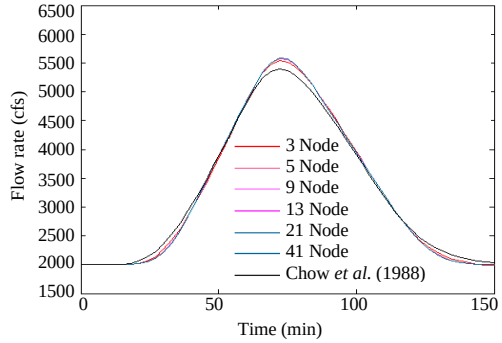

Fig. 3: Flow rate at point 12000 ft obtained by Newton-Raphson PIM; Newton PIM at node 12000 ft

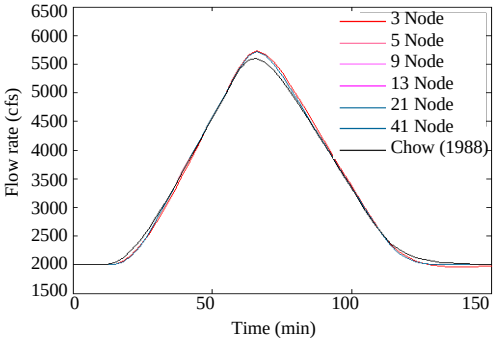

Fig. 4: Flow rate at point 6000 ft obtained by Picard PIM; Newton PIM at node 6000 ft

Figure 7-9 show the plot of discharge (flow rate) calculated using Newton-Raphson iterative scheme and Picard scheme, respectively. Based on the close agreement between the results, it can be concluded that PIM formulation has been verified for the case of flow driven by precipitation.

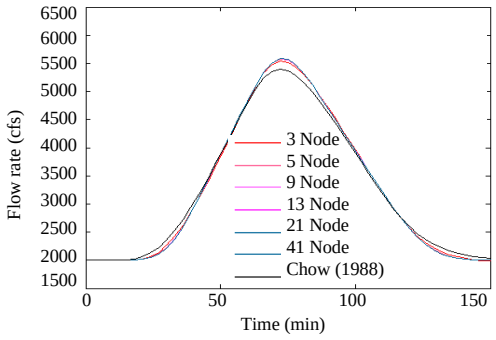

Fig. 5: Flow rate at point 12000 ft obtained by Picard PIM; Newton PIM at node 12000 ft

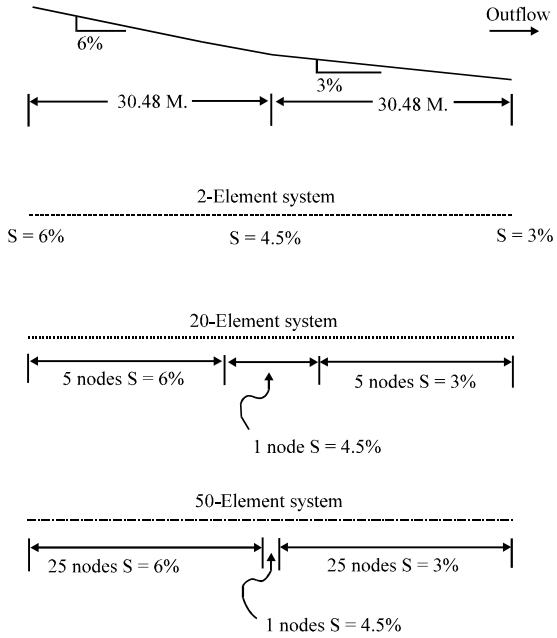

Fig. 6: One-dimensional element representation of two plane watershed; Vieux *et al.* (1990)

Case 3: Verification against gauged (real) data Litrico *et al.* (2010): In contrast to the two previous hypothetical works, Litrico *et al.* (2010) dealt with real data, gauged from Jacui River in Brazil. The flow was driven by time-varying upstream boundary conditions (varying inflow) as shown in Fig. 10. The data consisted of propagation of dam release on the Jacui River in Brazil between Itauba and Volta Grande, recorded at a time step of 30 min. Table 2 gives the data for the river.

Figure 11 and 12 show the plot of discharge (flow rate) calculated using Newton-Raphson iterative scheme and Picard scheme, respectively. Close approximations are evident between the plots hence the validation of the formulation and the corresponding source code.

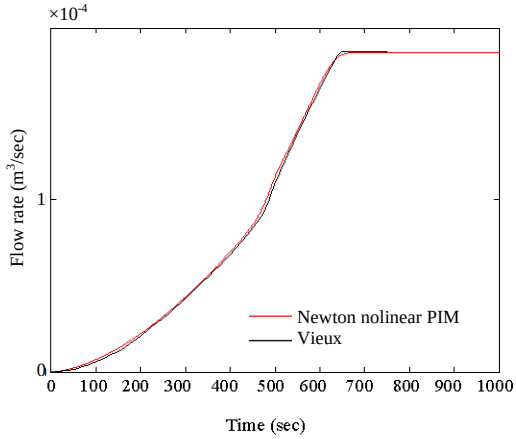

Fig. 7: Flow rate of PIM Newton-Raphson versus Vieux *et al.* (1990); Sollution comparison for 51 node

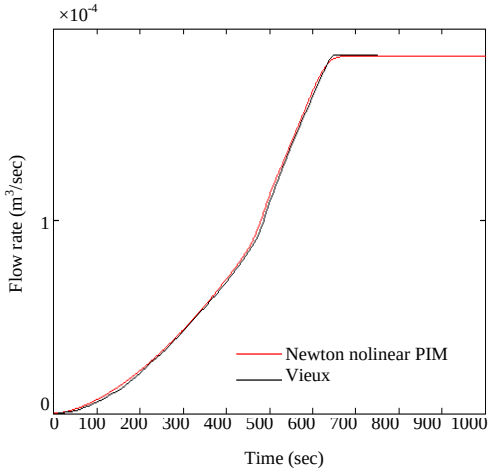

Fig. 8: Flow rate of PIM Picard versus Vieux *et al.* (1990); Sollution comparison for 51 node

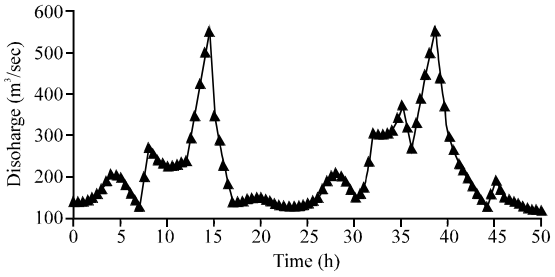

Fig. 9: Upstream flow; Litrico *et al.* (2010)

Table 2: Parameter of the study by Litrico *et al.* (2010)

Parameters	Values
Channel Length (L)	29600 m
Width (W)	55.6 m
Manning coefficient (n)	0.07
Slope (Sb)	0.00089

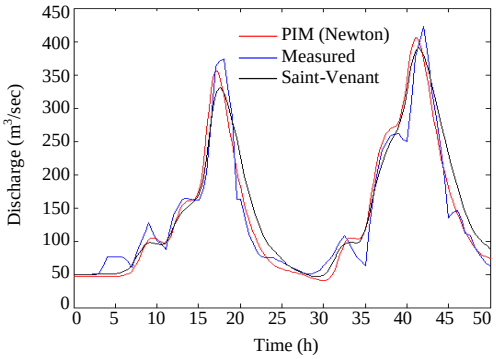

Fig. 10: PIM Newton-Raphson versus gauged and predicted data by Litrico *et al.* (2010)

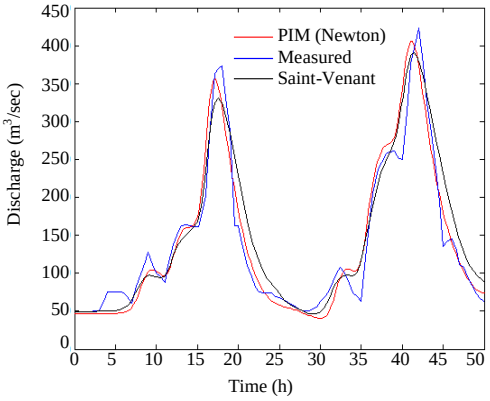

Fig. 11: PIM picard versus gauged and predicted data by Litrico *et al.* (2010)

CONCLUSION

This study has derived the PIM formulations for kinematic wave equation for flood routing. It provides detailed derivation of the weak statement of the problem as well as the derivation of the PIM shape functions and their first derivative. The final form of the formulation is thus given in numerical integration form as it suits the numerical nature of the PIM shape functions which are given only at the point of interest which in this case, taken at Gauss quadrature points. In the formulations, both nonlinear schemes are considered; Picard and Newton-Raphson. The formulation are verified against both hypothetical data obtained from conventional numerical methods (finite difference method and finite element method) and gauged data obtained from an actual river. Close agreements are obtained between the proposed PIM formulation and the conventional methods thus highlight the potential of PIM as an alternative numerical method in the field of hydrologic modelling.

REFERENCES

Chow, V.T., D.R. Maidment and L.W. Mays, 1988. Applied Hydrology. McGraw-Hill, New York, USA., ISBN:9780071001748, Pages: 572.

Govindaraju, R.S., M.L. Kavvas and S.E. Jones, 1990. Approximate analytical solutions for overland flows. Water Resour. Res., 26: 2903-2912.

Govindaraju, R.S., S.E. Jones and M.L. Kavvas, 1988. On the diffusion wave model for overland flow: 1 solution for steep slopes. Water Resour. Res., 24: 734-744.

Hjelmfelt, A.T., 1981. Overland flow from time-distributed rainfall. J. Hydraulics Div., 107: 227-238.

Litrico, X., J.B. Pomet and V. Guinot, 2010. Simplified nonlinear modeling of river flow routing. Adv. Water Resourc., 33: 1015-1023.

Liu, G.R. and Y.T. Gu, 1999. A point interpolation method. Proceedings of the 4th Asia-Pacific Conference on Computational Mechanics, December 13-15, 1999, Elsevier, Singapore, pp: 1009-1014.

Liu, G.R. and Y.T. Gu, 2003. A matrix triangularization algorithm for the polynomial point interpolation method. Comput. Methods Appl. Mech. Eng., 192: 2269-2295.

Liu, G.R. and Y.T. Gu, 2004. Boundary mesh free methods based on the boundary point interpolation methods. Eng. Anal. Boundary Elem., 28: 475-487.

Liu, G.R., Y.T. Gu and K.Y. Dai, 2004. Assessment and applications of point interpolation methods for computational mechanics. Int. J. Numer. Methods Eng., 59: 1373-1397.

Parlange, J.Y., C.W. Rose and G. Sander, 1981. Kinematic flow approximation of runoff on a plane: An exact analytical solution. J. Hydrology, 52: 171-176.

Singh, V.P., 2003. Kinematic wave modeling in hydrology. Proceedings of the ASCE Conference on World Water and Environmental Resources Congress, June 23-26, 2003, ASCE, Philadelphia, Pennsylvania, pp: 1-38.

Vieux, B.E., V.F. Bralts, L.J. Segerlind and R.B. Wallace, 1990. Finite element watershed modeling: One-dimensional elements. J. Water Resour. Plann. Manage., 116: 803-819.